WATER RESOURCES RESEARCH, VOL. 34, NO. 4, PAGES 777–785, APRIL 1998

A soil moisture–rainfall feedback mechanism
2. Numerical experiments

Xinyu Zheng and Elfatih A. B. Eltahir

Ralph M. Parsons Laboratory, Department of Civil and Environmental Engineering, Massachusetts Institute of Technology, Cambridge

Abstract. Here we develop a numerical model to investigate the hypothesis proposed by a companion paper [*Eltahir*, this issue], which describes a soil moisture–rainfall feedback mechanism. The model is designed to describe the seasonal evolution of the West African monsoon rainfall and is used to perform numerical experiments that elucidate the mechanisms of the response of rainfall to soil moisture anomalies. A significant rainfall anomaly is simulated by the model in response to a hypothetical soil moisture anomaly that has been imposed during early summer. However, the magnitude of this anomaly almost vanishes when the net radiation at the surface is not allowed to respond to the soil moisture anomaly. Hence the results of the numerical experiments support the proposed hypothesis and highlight the crucial importance of the radiative and dynamical feedbacks in regulating the rainfall anomalies that result from the soil moisture anomalies.

1. Introduction

In a companion paper by *Eltahir* [this issue] (hereafter ETI), a hypothesis has been proposed to describe a soil moisture–rainfall feedback mechanism. This hypothesis emphasizes the radiative feedbacks induced by anomalous wet soil moisture conditions which tend to increase the net radiation at the surface and the total heat flux from the surface into the atmosphere. Thus the moist static energy (or entropy) in the boundary layer is also likely to be enhanced. The increase of the boundary layer moist static energy is likely to increase the frequency and magnitude of local convection and strengthen the large-scale circulation and therefore result in more rainfall. ETI presented some observational evidence from FIFE data, which were collected in Kansas. The data suggest that wet soil moisture conditions are associated with smaller surface albedo and smaller Bowen ratio, both contributing to an increase in net surface radiation. In addition to that, the data also show that wet soil conditions are associated with larger total heat flux from the surface and hence larger boundary layer moist energy (which can be measured by wet bulb temperature). It was argued in ETI that the enhancement of moist static energy in the boundary layer and the associated lowering of the cloud base level could possibly result in more rainfall, by increasing the frequency and magnitude of local convection and by intensifying large-scale circulations (such as monsoons).

One of the caveats of the results presented in ETI is that the data used in that analysis are limited in their spatial coverage (covering a domain of 15 km $\times$ 15 km). Whether or not those observations are typical for other locations remains to be seen. Since simultaneous global observations of soil moisture and other land or boundary layer variables (e.g., radiative fluxes and heat fluxes) are yet to be available, numerical models of various complexities are alternative tools to study the soil moisture–rainfall feedback. Although the concepts of ETI are general, we here try to use a simple numerical model of West African monsoons as a platform to test and illustrate those concepts. The simple formulation of the model used in this study allows us to isolate the role of some important physical processes. This will helps us in identifying the dominant pathways in relating soil moisture and subsequent rainfall. In particular, we will investigate how significant is the mechanism proposed by ETI in comparison to other possible mechanisms such as those based on water balance and the concept of precipitation recycling.

The modeling studies on the soil moisture–rainfall feedbacks can be classified into three groups. The first group of studies is based on the concept of water balance [*Lettau et al*., 1979; *Eltahir*, 1989; *Rodriguez-Iturbe et al*., 1991; *Savenije*, 1995]. Although these water balance models are useful in illustrating the statistical nature of the soil moisture–rainfall feedback, these same models fail to consider other important feedback processes associated with soil moisture dynamics, namely, those involving the surface energy balance and dynamical processes that couples boundary layer conditions and rainfall. The second group of studies takes into account the coupling between the land surface and the turbulent boundary layer where the energy balance is included. For example, *Sasamori* [1970], *Zdunkowski et al*., [1975], and *Raddatz* [1993] developed numerical models of the boundary layer to address the interaction between the land surface and the planetary boundary layer. However, these models simply do not include any explicit rainfall mechanisms such as deep moist convection. Furthermore, these models do not incorporate any feedbacks between the free atmosphere and the boundary layer. These two groups of studies focus mainly on local land-atmosphere interactions. Finally, there are studies concerned with the response of atmospheric circulation to soil moisture anomalies, including those on the excitation of mesoscale thermally direct circulations caused by mesoscale land surface soil moisture heterogeneities [e.g., *Segal and Arritt*, 1992] and those on the large-scale circulation changes due to large-scale soil moisture anomalies [e.g., *Walker and Rowntree*, 1977; *Yeh et al*., 1984]. In general, these studies demonstrate that soil moisture anomalies are able to cause significant subsequent rainfall variability. In particular, *Walker and Rowntree* [1977] showed that dry and

Paper number 97WR03497.
0043-1397/98/97WR-03497$09.00

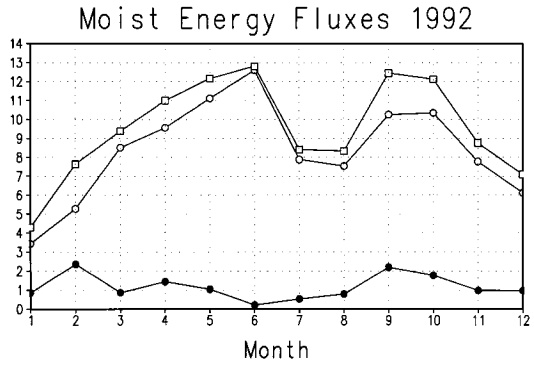

Figure 1. The seasonal evolution of the net vertically integrated moist static energy fluxes into the region of study, scaled by the area of the region (15°E, 5°N to 20°), for 1992. The solid circles indicate the net flux across the eastern-western boundaries; the open circles indicate the net across northern-southern boundaries; the squares indicate the total net fluxes. Positive values mean the net convergence of moist static energy flux. The unit is 10^3 W m^{-2}.

wet soil moisture conditions can persist through seemingly positive feedback between soil moisture and rainfall. However, their model integration may be too short (~10–20 days) for their results to be conclusive. More importantly, their study did not include the radiative feedback caused by different soil moisture anomalies, which we identify here as an important pathway in the soil moisture–rainfall feedback process. Our study here will emphasize the role of radiative processes in the dynamics of the soil moisture–rainfall interaction. We are interested mainly in modeling the rainfall response to large-scale soil moisture anomalies. Unlike general circulation models (GCMs), our model is designed to focus on a subset of the important processes related to West African monsoon rainfall instead of simulating all the details of the real atmosphere. However, the model has the advantages of conceptual simplicity and computational efficiency.

The paper is organized as follows. We first describe the model in detail and compare the model simulations against observations (section 2). Then we perform some numerical experiments to examine the model response to soil moisture anomalies (section 3). Finally, we summarize our conclusions and remarks (section 4).

2. Model Description and Control Experiment

2.1. Model Description

We are interested in rainfall variability on timescales longer than a month. Hence the effect of zonal asymmetries, which has shorter timescales, is assumed to be negligible in describing West African monsoons. This assumption is further justified by observations that indicate that vegetation, temperature, specific humidity, and rainfall in West Africa are indeed uniform in the zonal direction. In the following we focus on moist static energy as an example for important atmospheric variables, to illustrate the validity of the zonal symmetry assumption. For the West African region, defined as from 15°W to 15°E, and from 5°N to 20°N, we analyzed the net vertically integrated moist static energy flux convergence for the dry year of 1992 and the wet year of 1994 (these are the driest and wettest years in 1990s [*Nicholson et al.*, 1996]) using ECMWF (European Centre for Medium-Range Weather Forecast) data. In so doing, the results should be representative for the typical West African climate.

Figures 1 and 2 show the seasonal evolution of net moist static energy flux convergence for 1992 and 1994, respectively. It is evident that during the summer, which is the rainy season in West Africa, the meridional (north-south) flux convergence is dominant over the zonal (east-west) flux convergence. Similar analyses have also been performed for water vapor as well as momentum. The results (not shown here) also show that the effects of zonal asymmetries on both water vapor and momentum are of secondary importance. For water vapor, zonal asymmetries account for a maximum of 30% of the total observed net water vapor convergence. In addition, zonal asymmetries contribute a net water vapor divergence out of the West African region, suggesting that the omission of zonal asymmetries probably will overestimate the net moisture convergence into the West African region. This issue will be discussed later when we compare our model control experiment with observations. Hence, to the zeroth order, the effect of zonal asymmetries can be ignored; the adoption of the zonally symmetric (no zonal variations) dynamical framework is justified.

In reality, zonal asymmetries such as easterly waves are the actual rain-producing systems. Our model is not capable of simulating these individual disturbances. Our objective here is to simulate the collective effect of these zonal asymmetries. Clearly, the timescale of our interest is much longer than the life cycle of individual disturbances. Moreover, the model is designed as a process model so that we are not trying to simulate the detailed variability in the natural system. Instead, a limited set of essential processes is included in order to investigate the essential physical processes that may be important for simulating realistic West African monsoon rainfall.

This model has been used in previous studies to investigate the impact of vegetation degradation and sea surface temperature on West African rainfall [*Zheng and Eltahir*, 1998; X. Zheng et al., A mechanism relating tropical Atlantic spring sea surface temperature and west African rainfall, submitted to *Quarterly Journal of the Royal Meteorological Society*, 1997, herein after referred to as submission]. However, for the sake of completeness, we give a detailed description of the model in this section. The model domain represents a longitudinally averaged (from 15°W to 15°E) latitude-height cross section. The model domain is global horizontally and extends from the surface up to 25 km in log pressure coordinates. The grid points are evenly spaced in sine latitude horizontally with 46 increments (about 2.5° resolution in terms of latitude in trop-

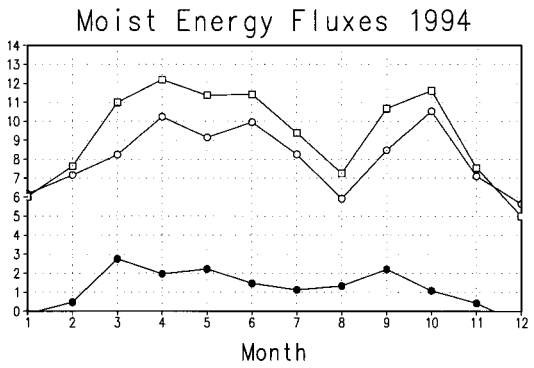

Figure 2. The same as Figure 1 but for 1994.

ics) and also equally spaced vertically with 25 increments (1 km vertical resolution). The time step is 20 min.

The model surface consists of a land surface north of 5°N (which is assumed to be the location of the southern Atlantic coast) and an ocean surface south of 5°N. The sea surface temperature (SST) data used here are taken from the monthly optimum interpolation (OI) SST analysis [*Reynolds and Smith*, 1994]. The data cover the whole globe and have a spatial resolution of 1° × 1°. The time coverage is from January of 1981 to December of 1995.

The model uses primitive momentum equations. An explicit hydrological cycle is incorporated. Hydrostatic approximation is assumed since we are interested only in large-scale circulations (see work by X. Zheng (submission) for details of the model dynamical framework as well as the model numerical schemes). We use a fast radiation parameterization developed by *Chou et al*. [1991] which combines the schemes of *Chou* [1984], *Chou and Peng* [1983], *Rodgers* [1968], *Lacis and Hansen* [1974], *King and Harshvardhan* [1985], and *Joseph et al*. [1976]. For the experiments described here and for simplicity we assume clear sky conditions for radiation calculations. The implications of this assumption are discussed in the concluding remarks section. Above the model top (25 km, about 38.8 mbar), we add 9 layers up to 1 mbar in radiative equilibrium.

The ensemble effect of moist convections (both deep and shallow) is parameterized by the Emanuel scheme [*Emanuel*, 1991]. This scheme is a physically based parameterization which takes account of current available theories, observations, and results of numerical simulations. On the basis of observations of inhomogeneity of individual convective clouds, the basic assumption of this scheme is that the fundamental convecting entities are those subcloud-scale ($O(100\text{m})$) updrafts and downdrafts rather than the clouds themselves. The main closure parameters are parcel precipitation efficiency, which determines the fraction of condensed water in a parcel lifted to any level that is converted to precipitation; the fraction of precipitation that falls through unsaturated air; and the fractional area covered by the precipitating downdrafts. These three parameters represent the microphysical processes responsible for determining how much condensed water reevaporates, thus moistening and cooling the air, and how much falls out of the system, leading to warming and drying. Thus this scheme directly relates the large-scale temperature and moisture tendencies to microphysical parameters. The scheme produces large-scale tendencies (ensemble effect of moist convection) of temperature and specific humidity by using the profiles of temperature and specific humidity as input.

The prognostic equation of land surface temperature follows *Srinivasan et al*. [1993]:

$$C_E \frac{\partial T_g}{\partial t} = R_{\text{net}} - H - L_v E, \tag{1}$$

where $C_E = 4.5 \times 10^6$ J m^{-2} K^{-1} is the effective volumetric heat capacity of soil per unit area; T_g is ground temperature; t is time; R_{net} is surface net radiative flux; H is surface sensible heat flux; $L_v E$ is surface latent heat flux; L_v is latent heat of vaporization; and E is surface evaporation.

We use the *Budyko* [1974] climate index of dryness as the indicator of the vegetation type. The vegetation type basically determines the depth of the root zone and therefore the size of the soil moisture reservoir. We assume a latitudinal distribution of the dryness index, mimicking the actual natural vegetation distribution in West Africa qualitatively. In general, the dryness index has a small value (less than 1) within the tropical forest region and increases northward, achieving a maximum (greater than 3) in the desert region [*Budyko*, 1974]. This dryness index pattern roughly depicts the transition of the vegetation type in West Africa, from tropical forest near the southern Atlantic coast to the semiarid plants (grasslands, shrubs) in Sahel and the Sahara desert. The analytical form of the assumed dryness index is

$$\begin{aligned} D &= 0.5 \qquad \phi_0 \le \phi \le \phi_1 \\ D &= 3.7 + (3.7 - 0.5)\,\frac{\phi - \phi_1}{\phi_2 - \phi_1} \qquad \phi_1 \le \phi \le \phi_2 \\ D &= 3.7 \qquad \phi > \phi_2 \end{aligned} \tag{2}$$

where ϕ is latitude; $\phi_0 = 5°$ (coast line), $\phi_1 = 10°$N, and $\phi_2 = 20°$N. We follow *Gutman et al*. [1984] and relate the field capacity W_c to the dryness index D:

$$W_c = W_0 \frac{\tanh D}{D} \qquad D \ge 0 \tag{3}$$

where $W_0 = 80$ cm [*Dickinson et al*., 1986]. This simply means that the maximum soil moisture capacity depends on the vegetation type (depth of the root zone), as indicated by the dryness index here. It should be pointed out that the specification of the field capacity may affect the persistence timescale of the soil moisture [*Milly and Dunne*, 1994].

A simple soil hydrology scheme is included in this model, we use the bucket model of *Manabe* [1969]. What is different here is that our field capacity has latitudinal variation whereas for *Manabe* [1969] the field capacity was held constant everywhere. The soil moisture prognostic equation is

$$\begin{aligned} \frac{\partial W}{\partial t} &= 0 \qquad W \ge W_c,\ P \ge E \\ \frac{\partial W}{\partial t} &= P - E \qquad \text{otherwise} \end{aligned} \tag{4}$$

where P is precipitation and E is evaporation. Any excessive soil moisture above field capacity is considered as runoff. The evaporation is evaluated according to the relative saturation of soil moisture and potential evaporation E_p, which is parameterized by a bulk formula (drag coefficients are 1.0×10^{-3} for the ocean and 2.0×10^{-3} for the land):

$$E = E_p \left(\frac{W}{W_c} \right)^{\beta} \tag{5}$$

where β is taken to be 1.

The recent observations from ERBE (Earth Radiation Budget Experiment) indicate that the surface albedo (α) of West Africa has a zonally uniform distribution [*Darnell et al*., 1995], supporting our use of the zonally symmetric model. In addition, the surface near Sahara desert was found to be highly reflective (as high as 48%). Here we assume an analytical form of the relationship between the albedo and the dryness index to mimic the observed albedo pattern:

$$\begin{aligned} \alpha &= \min\,(0.48,\ 0.014 + 0.126D) \qquad D \ge 1 \\ \alpha &= 0.14 \qquad 0 < D < 1 \end{aligned} \tag{6}$$

Note that within the tropical forest region (defined as $0 < D < 1$), there is no dependence of the surface albedo on the

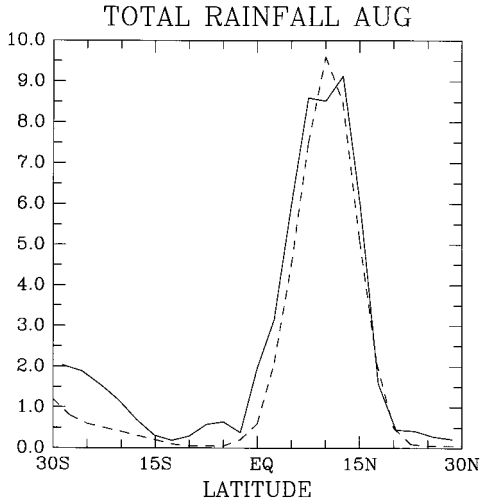

Figure 3. The latitudinal profile of the total rainfall in August for control experiment (solid line) versus the observed 1987–1994 GPCP August climatology (dashed line), averaged from 15°W to 15°E.

dryness index [*Gutman et al*., 1984]. Moreover, we also take into account the effect of soil moisture on the surface albedo by multiplying the surface albedo defined above by a factor $(1 - 0.5(W/W_c))$ for all regions except tropical forest regions, where the albedo is held as 0.14. This means that the saturation of the soil can decrease the albedo defined in (3) by 50% for fully saturated soil. The oceanic surface albedo is taken as 0.06.

2.2. Control Experiment

The control experiment is forced by SST climatology from 1981 to 1995. The solar forcing has a seasonal cycle (no diurnal cycle). The model is first integrated for 300 days by fixing the solar insolation at the spring equinox. This creates the initial state for subsequent runs with seasonally varying solar insolation. Then the model is integrated long enough (about 2–3 years) to produce equilibrium, which is used as our control atmosphere.

Here we try to compare the results from the control experiment with the observations. The rainfall data are based on GPCP (Global Precipitation Climatology Project) products. This data set provides monthly mean 2.5° × 2.5° gridded precipitation data for the period July 1987 through December 1994 (December of 1987 is missing). The data set has been produced by blending rain gauge observations, satellite-based (infrared and microwave) estimates of precipitation, and NWP (National Weather Prediction) model precipitation information [*Huffman et al*., 1995].

Figure 3 shows the latitudinal distributions of total rainfall in August. The rainfall distribution in the control experiment agrees reasonably well with that of the observations, in terms of the location of rainfall maximum (ITCZ) as well as the north-south gradient of rainfall. In addition, the seasonal cycle of the rainfall over Sahel (10°N to 20°N) exhibits similarity to the observations (Figure 4). For example, rainfall achieves maximum in August as observed. However, the model overestimates rainfall most of the year, probably because of the neglect of zonal asymmetries. As we mentioned earlier, the effect of zonal asymmetries on moisture budget over West Africa is a net moisture divergence out of West Africa. Our zonally symmetric model ignores this effect and therefore can exaggerate moisture convergence and hence rainfall.

Figure 5 shows the comparison between the model net radiation at the surface and that of the ERBE observation [*Darnell et al*., 1995] for the month of June, when we will introduce soil moisture anomalies (see section 3). This is meant to give a general idea about how the model surface radiation compares to the observation since these two curves are not completely comparable. The observation is just for one particular year (1990, averaged from 15°W to 15°E), whereas our model results describe a climatology for the period 1981–1995. In general, the model does a reasonable job, although there is a substantial deviation north of 20°N.

The relative saturation of soil moisture (ratio between actual soil moisture and field capacity) for the control experiment

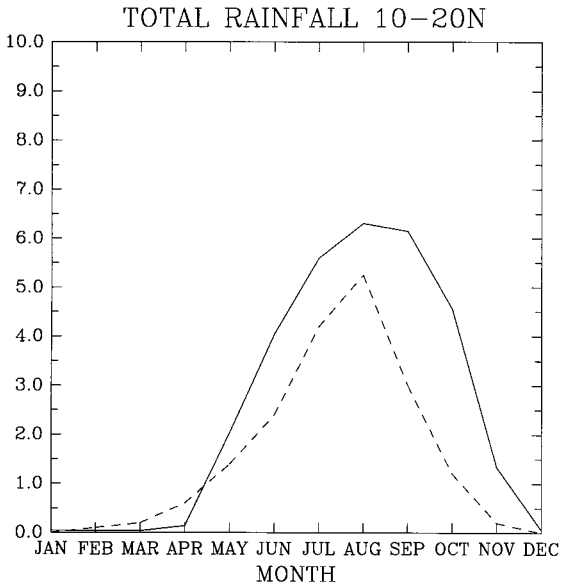

Figure 4. The time series of the total rainfall over the region from 10°N to 20°N for the control run (solid line) and the observed 1988–1994 GPCP rainfall climatology (dashed line).

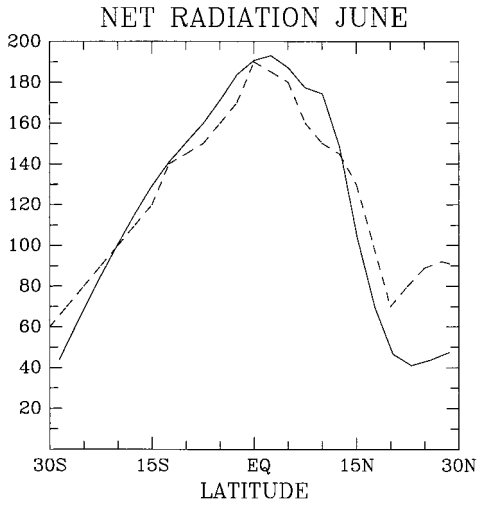

Figure 5. The net surface radiation in June. The solid line is the model output; the dashed line is the ERBE data.

shows that soil is relatively dry in spring after a period of deficient rainfall in winter and wet in late summer and early fall following summer rainy season (Figure 6). Unfortunately, observations on soil moisture are not available for comparison.

3. Numerical Experiments

3.1. Design of the Experiments

Our objective here is to use the model described in section 2 as a tool to test the hypothesis proposed in ETI regarding the soil moisture–rainfall feedback. In particular, we focus on the role of soil moisture conditions in influencing the surface radiation budget and large-scale monsoon circulation. First, we introduce a soil moisture anomaly south of 20°N on June 1 (day 152 in Figure 6) to the control experiment such that the actual soil moisture W is given by $W = W_{\text{control}} + \gamma(W_c - W_{\text{control}})$, where W_c is the field capacity, W_{control} is the soil moisture for the control state, γ is an adjustable parameter, which here we take as 0.25. Note that $\gamma = 1$ means saturating the soil. This experiment essentially "irrigates" the soil by 25% of the soil moisture deficit. After this sudden "irrigation" the atmosphere is allowed to respond radiatively and dynamically. Also, the soil moisture is allowed to interact with rainfall. Therefore this experiment includes interactions through both energy and water cycles. We refer to this experiment as the fully interactive case. It should be pointed out that the magnitude and spatial pattern of the soil moisture anomaly we introduce here have no observational evidence. Our objective is to investigate the model sensitivity to a hypothetical soil moisture anomaly and then to use the results of these experiments to examine the validity of the hypothesis proposed by ETI.

The second experiment is designed to isolate the role of surface radiative fluxes in the soil moisture–rainfall feedback. In this experiment we fix all the surface radiative fluxes (net longwave flux, net shortwave flux and net total radiative flux) exactly the same as the values in the control experiment after introducing the same soil moisture as the fully interactive experiment on June 1. In other words, this experiment does not allow any changes in surface radiation budget in response to the soil moisture anomaly. However, other interactions and in particular those involving the water balance of the hydrological cycle are allowed. We refer to this experiment as the fixed radiative flux case.

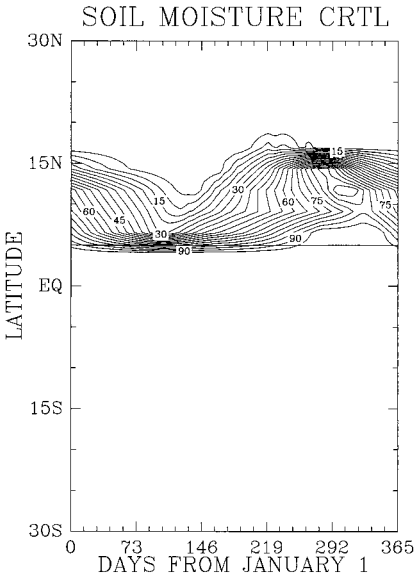

Figure 6. The relative soil moisture (ratio between soil moisture and field capacity) latitude-time cross section for the control case; contour interval is 5%.

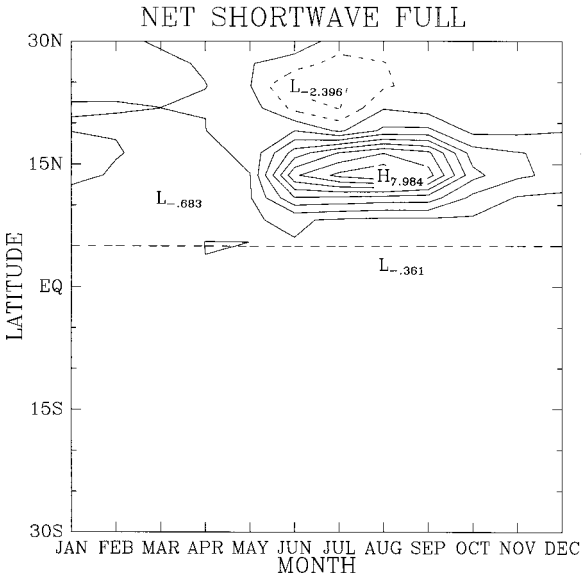

Figure 7. The net surface shortwave radiation anomaly, for the fully interactive experiment. The contour interval is 5 W m^{-2}.

The philosophy in designing these experiments is simple: the fully interactive experiment basically includes all possible feedback processes described in the model. However, in the fixed radiative flux experiment we artificially eliminate surface radiative feedback processes that may result from the soil moisture anomalies. By comparing the results of this experiment with those of the fully interactive case, we will evaluate the net impact of surface radiative fluxes on the soil moisture–rainfall feedback.

3.2. Results

First, let us examine the fully interactive experiment, starting from surface radiation budget. The hypothesis described in ETI predicts that wetter soil should decrease surface albedo and therefore increase surface shortwave radiation. In addition, a wetter soil cools the land surface temperature and increases atmospheric water vapor content through larger evaporation (hence larger greenhouse effect). Therefore the surface net longwave radiation should also be enhanced. For the fully interactive experiment, indeed we observe larger net shortwave radiation and net longwave radiation (Figures 7 and 8) compared to the control experiment, over the region of soil moisture anomaly. Accordingly, the net surface radiation is also enhanced (Figure 9). Consistent with the change of surface radiation fluxes, the total heat flux from the surface also increases (Figure 10). Associated with this, we observe a dominant positive anomaly of boundary layer moist static energy (Figure 11), although a slight decrease occurs from 5°N to 10°N. This slight decrease happens in a region of wetter soil moisture conditions, seemingly against the hypothesis in ETI. However, as pointed out by *Emanuel* [1995], the existence of monsoon circulation modifies the distribution of boundary layer moist static energy. The larger heat flux–larger moist

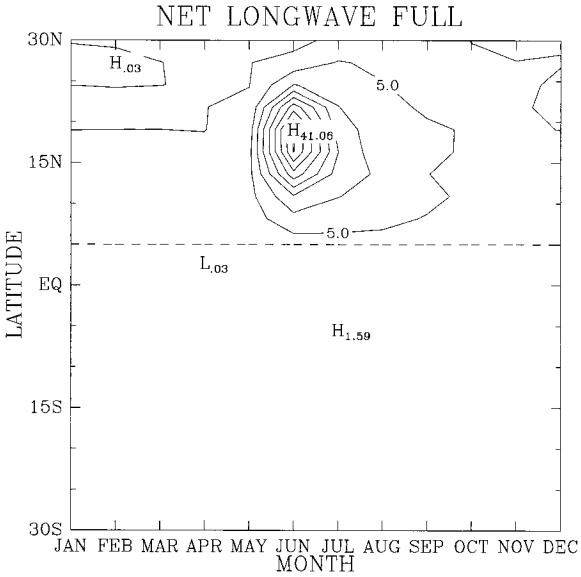

Figure 8. The net surface longwave radiation anomaly, for the fully interactive experiment. The contour interval is 5 W m^{-2}.

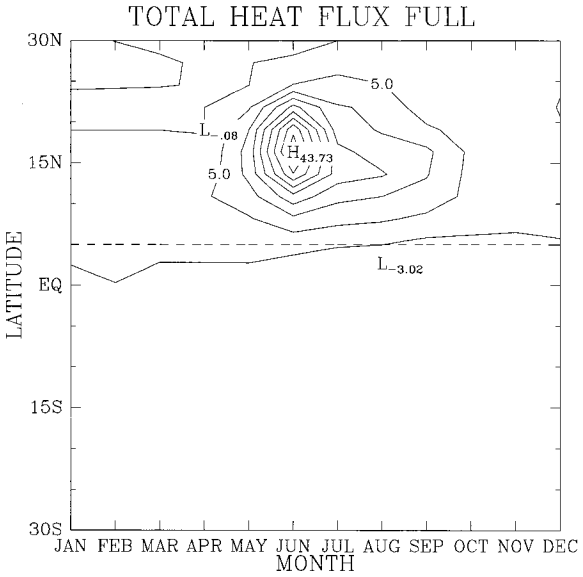

Figure 10. The anomaly of the total heat flux from the surface, for the fully interactive experiment. The contour interval 10 W m^{-2}.

static energy argument in ETI is one-dimensional thinking. In other words, no dynamics is involved in that argument. In general, wetter soil conditions cause changes in both rainfall and moist static energy through complicated radiative-dynamical feedbacks. These feedbacks induce changes in total rainfall (Figure 12), surface evaporation (Figure 13), and large-scale monsoon circulation. It should be mentioned that the location of maximum rainfall anomaly lies slightly south of the location of the maximum moist static energy. This is expected from the theories of zonally symmetric circulations [e.g., *Emanuel*, 1995]. This is because the location of the maximum moist static energy indicates the northernmost boundary of the monsoon circulation, and the maximum rainfall belt lies south of it.

Now if we artificially do not allow any changes in surface radiative fluxes to the initial soil moisture anomaly, as we did in the fixed radiative flux experiment, the increase of rainfall is substantially smaller than that of the fully interactive experiment (comparing Figure 14 with Figure 12). More importantly, we observe that the pattern of rainfall anomalies is much more elongated for the fully interactive case than that of the fixed radiative flux case. For example, for the fully interactive case (Figure 12) the 0.5 mm/d contour extends all the way up to October, whereas it is basically limited to June for the fixed radiative flux case (Figure 14). This difference indicates that the persistence time of the rainfall anomaly for the fixed radiative experiment is significantly shorter than that of the fully

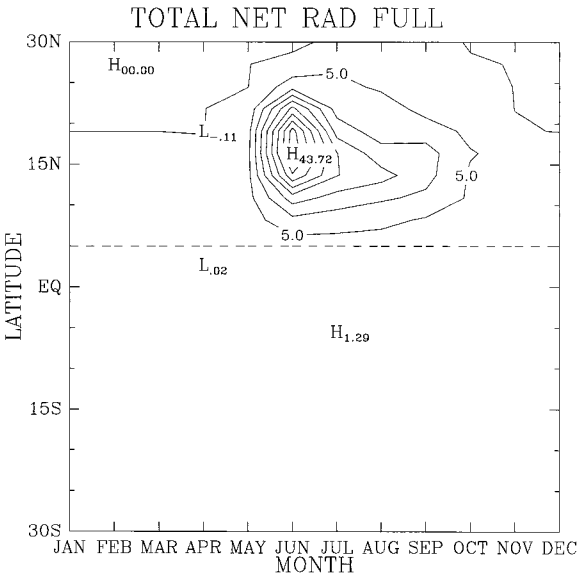

Figure 9. The total net surface radiation anomaly, for the fully interactive experiment. The contour interval 10 W m^{-2}.

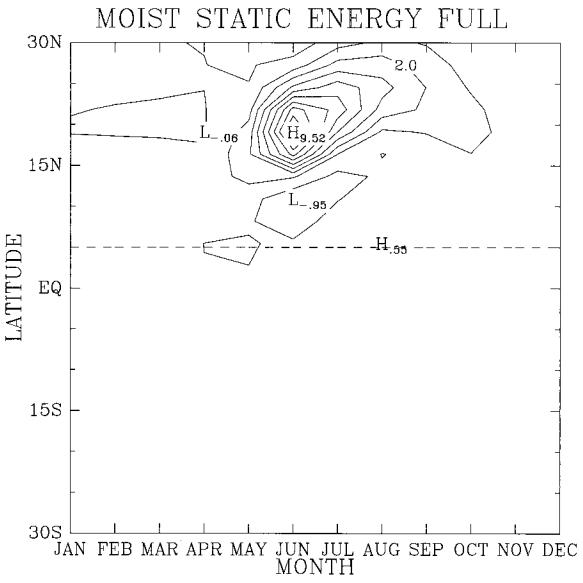

Figure 11. The boundary layer moist static energy anomaly, scaled by the heat capacity (units in Kelvins), for the fully interactive experiment. The contour interval 1.0 K.

interactive case. This experiment demonstrates the crucial importance of surface radiative fluxes in enhancing and sustaining the rainfall anomaly. We can see that the concept of recycling, when based only on water balance, oversimplifies the complex interactions that may lead to sustaining soil moisture and rainfall anomalies. In fact, our particular example here shows that disregarding the role of surface radiative fluxes significantly weakens the soil moisture–rainfall feedback, in terms of both the persistence time and the magnitude of rainfall anomalies.

In summary, the results of these two experiments confirm the critical importance of surface radiation budget in the soil moisture–rainfall feedback. According to ETI, this conclusion should not be surprising since surface net radiation determines the total heat flux from the surface as well as the boundary layer moist static energy, which is closely related to rainfall processes both at local scales and regional scales. Without the positive feedback due to surface radiative fluxes, the increase of rainfall due to wetter soil through pure water recycling is very small and short lived (Figure 14).

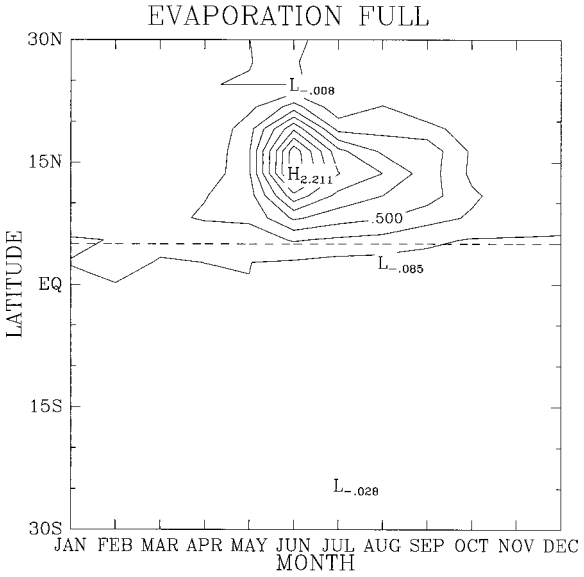

Figure 13. The surface evaporation anomaly, for the fully interactive experiment. The contour interval 0.5 mm/d.

4. Concluding Remarks

The results of the numerical experiments described in this paper point to the critical role of radiative processes in the soil moisture–rainfall feedback. Without the radiative feedback processes, we find that the rainfall anomaly caused by the initial soil moisture anomaly is significantly decreased. Our model results show that wet soil moisture conditions increase the net surface radiation and the total heat flux from the surface. Therefore larger boundary layer moist static energy (or entropy) has been simulated for relatively wet soil moisture conditions. The increase of boundary layer moist static energy has two possible effects. At local scales the larger moist static energy favors larger rainfall [*Williams and Renno*, 1993; *Eltahir and Pal*, 1996]. At larger scales the increase of boundary layer moist energy is also likely to strengthen the large-scale monsoon circulation by enhancing the gradient of moist static energy [*Eltahir and Gong*, 1996; *Emanuel*, 1995]. For the example considered in this paper the increase of rainfall is mainly due to the increase of local evaporation, as can be seen by comparing Figure 12 with Figure 13. The circulation effect is secondary. However, the relative importance of changes in local evaporation and changes in large-scale circulation may be different for different situations. In principle, wet soil moisture conditions could cause changes in both local evaporation and large-scale convergence.

The hypothesis proposed in ETI describes the feedbacks caused by wet/dry soil moisture conditions and emphasizes the radiative and dynamical response induced by soil moisture anomalies. Here observational evidence has been presented to show that wetter soil is indeed associated with smaller surface albedo and smaller Bowen ratio. These contribute to the enhancement of surface net radiation and hence total heat flux

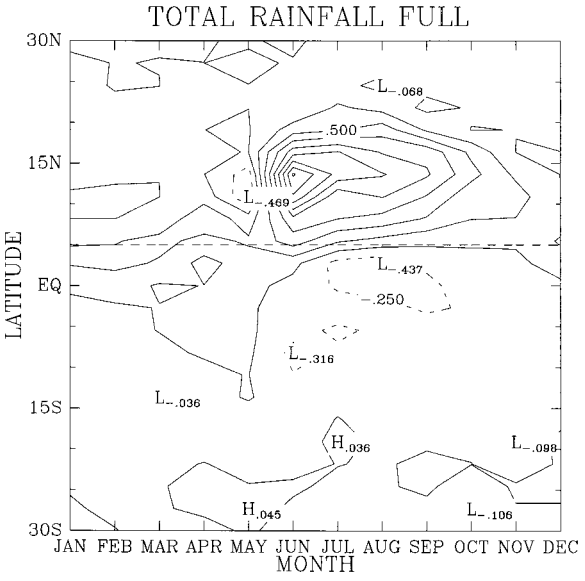

Figure 12. The total rainfall anomaly, for the fully interactive experiment. The contour interval 0.5 mm/d.

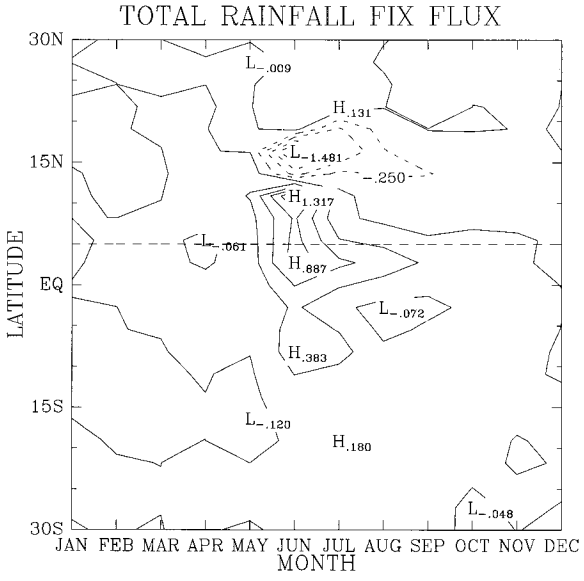

Figure 14. The total rainfall anomaly, for the fixed radiative flux experiment. The contour interval 0.5 mm/d.

from the surface. The increase of total heat flux then induces larger boundary layer moist static energy which in turn increases rainfall by increasing both local evaporation and large-scale moisture convergence. Our numerical experiments illustrate this chain of feedback processes. Most importantly, the energy-related and radiative feedbacks, which did not receive enough attention by previous studies, are identified to be critical for shaping the soil moisture–rainfall feedback.

We have to caution here that the objective of this paper is more illustrative than conclusive. We use a simple model of West African monsoons to elucidate some basic concepts in the hypothesis of ETI. We identify some dominant pathways of soil moisture–rainfall feedback, namely, the crucial importance of energy processes (radiative feedback involving surface fluxes, in particular). Obviously, the magnitude of rainfall anomalies depends on the magnitude of soil moisture anomalies and the details of the parameterizations. The larger the initial soil moisture anomaly, the larger the rainfall anomaly. Quantitative details of our experiments should not be considered too seriously because no soil moisture data are available and our model may be too simple to simulate the detailed features of the natural system. Nevertheless, we believe the results of these experiments illustrate the mechanism of the soil moisture–rainfall feedback proposed by ETI.

There are potential uncertainties in our study. The model assumes a constant depth for the boundary layer. As a result, several of the important processes that are described by ETI are not represented in this model. For the sake of simplicity we deliberately shut down the cloud-radiation feedback. However, the qualitative effect of cloud radiation is not hard to assess. Changes of net surface radiation due to wet soil moisture conditions consist of the change in net shortwave radiation and the change in net longwave radiation. For the shortwave component, wet soil moisture conditions increase cloudiness in general and thus allow less incoming solar radiation. This feedback works against the decrease of surface albedo following wet soil moisture conditions. Therefore the inclusion of cloud-radiation feedback would tend to cancel the effect of surface albedo. Hence we expect smaller increase of net shortwave radiation at the surface when cloud-radiation feedback is considered. On the other hand, more cloudiness permits less longwave radiation to escape into outer space and results in larger increase of net surface longwave radiation. In short, the inclusion of cloud-radiation feedback may change the relative contribution to the change in net surface radiation from shortwave and longwave components; that is, there is a larger increase of net surface longwave radiation and smaller increase of net surface shortwave radiation compared to cases without cloud-radiation feedback, such as the numerical experiments in this paper. The mechanism proposed in ETI has been recently corroborated by C. Schär et al. (The soil-precipitation feedback: A process study with a regional climate model, submitted to *Journal of Climate*, 1997), who studied the role of soil moisture in summer climate over Europe. Their model includes an interactive clouds scheme. Although the cloudiness feedback plays an important role in the partition of shortwave and longwave radiation at the surface in their model simulations; the essence of the proposed impact of soil moisture on net radiation remains unchanged.

This analysis of the role of clouds is consistent with the results of several GCM studies concerning vegetation degradation (e.g., Amazon deforestation). Note that vegetation has a role similar to soil moisture: Denser vegetation cover is associated with smaller surface albedo and more evaporation [*Eltahir*, 1996]. Deforestation corresponds to dry soil conditions. *Nobre et al*. [1991] estimated a 26 W/m^2 decrease of net surface radiation following a deforestation of large areas ($\sim 10^6$ km^2) in the Amazon. The decrease is composed of an 18 W/m^2 decrease in net shortwave radiation and an W/m^2 decrease in net longwave radiation. No cloud-radiation feedback was included in this study. The model of *Dickinson and Kennedy* [1992] included the cloud-radiation feedback. They reported an 18 W/m^2 decrease of net surface radiation for a similar area of deforestation. Of the total decrease of net surface radiation, now only 3 W/m^2 comes from the decrease in net solar radiation; the other 15 W/m^2 contribution is due to the decrease in net longwave radiation. We see clearly that even with the inclusion of cloud-radiation feedback, the net surface radiation still decreases following vegetation degradation although the magnitude is smaller, at least from these numerical model studies. *Lean and Rowntree* [1993] also reached a result similar to that of *Dickinson and Kennedy* [1992], again the cloud-radiation feedback was included. The decrease in net radiation is now mainly due to the decrease of net longwave radiation. Because of the analogy between soil moisture and vegetation cover, we expect similar effects for the cloud-radiation feedback following wet soil moisture conditions (opposite sign of course).

Finally, the soil moisture–rainfall feedback is also dependent on the convective parameterization, as demonstrated by *Pal and Eltahir* [1997] in a recent study on the droughts and floods of the U.S. Midwest. They compared two schemes: the Kuo scheme and the Grell scheme [*Giorgi et al*., 1993]. For the Kuo scheme, significant rainfall anomalies were found following initial soil moisture anomalies. On the other hand, for the Grell scheme, little sensitivity was detected against initial soil moisture anomalies. Our convective scheme here (the Emanuel scheme) is a physically based scheme and is more similar to the Grell scheme than to the Kuo scheme, which is highly unphysical [*Emanuel*, 1994]. Therefore the Emanuel scheme is expected to have a similar sensitivity to that of the Grell scheme. The fact that we still get substantial sensitivity of rainfall to soil moisture anomalies suggests that these results should not be altered qualitatively by using a different convection scheme.

Acknowledgments. The constructive comments by Alan Betts, Randy Koster, and one anonymous reviewer were helpful in preparing the final version of this paper. This research was supported by the MIT/ETH/University of Tokyo Alliance for Global Sustainability and by NASA under agreements NAGW-5201 and NAGW-4707.

References

Budyko, M. I., *Climate and Life*, *Int. Geophys. Ser*., vol. 18, 508 pp., Academic, San Diego, Calif., 1974.

Chou, M.-D., Broadband water vapor transmission functions for atmospheric IR flux computations, *J. Atmos. Sci*., *41*, 1775–1778, 1984.

Chou, M.-D., D. P. Kratz, and W. Ridgeway, Infrared radiation parameterizations in numerical climate models, *J. Clim*., *4*, 424–437, 1991.

Chou, M.-D., and L. Peng, A parameterization of the absorption in the 15 mm CO_2 spectral region with application to climate sensitivity studies, *J. Atmos. Sci*., *40*, 2183–2192, 1983.

Darnell, W. L., W. F. Staylor, S. K. Gupta, N. A. Ritchey, and A. C. Wilber, A global long-term data set of shortwave and longwave radiation budget, *GEWEX News*, *4*(3), 1–8, 1995.

Dickinson, R. E., A. Henderson-Sellers, P. J. Kennedy, and M. F. Wilson, Biosphere-Atmosphere Transfer Scheme (BATS) for the

NCAR Community Climate Model, *NCAR/TN-275 + STR*, 68 pp., 1986.
Dickinson, R. E., and P. Kennedy, Impacts on regional climate of Amazon deforestation, *Geophys. Res. Lett*., *19*(19), 1947–1950, 1992.
Eltahir, E. A. B., A feedback mechanism in annual rainfall, Central Sudan. *J. Hydrol*., *110*, 323–334, 1989.
Eltahir, E. A. B., The role of vegetation in sustaining large scale atmospheric circulations in the tropics, *J. Geophys. Res*., *101*(D2), 4255–4268, 1996.
Eltahir, E. A. B., A soil moisture–rainfall feedback mechanism, 1, Theory and observations, *Water Resour. Res*., this issue.
Eltahir, E. A. B., and C. Gong, Dynamics of wet and dry years in West Africa, *J. Clim*., *9*(5), 1030–1042, 1996.
Eltahir, E. A. B., and J. S. Pal, The relationship between surface conditions and subsequent rainfall in convective storms, *J. Geophys. Res*., *101*(D21), 26,237–26,245, 1996.
Emanuel, K. A., A scheme for representing cumulus convection in large-scale models, *J. Atmos. Sci*., *48*, 2313–2335, 1991.
Emanuel, K. A., *Atmospheric Convection*, 580 pp., Oxford Univ. Press, New York, 1994.
Emanuel, K. A., On thermally direct circulations in moist atmospheres, *J. Atmos. Sci*., *52*, 1529–1534, 1995.
Giorgi, F., M. R. Marinucci, and G. T. Bates, Development of a Second-Generation Regional Climate Model (RegCM2), II, Convective processes and assimilation of lateral boundary conditions, *Mon. Weather Rev*., *121*, 2814–2832, 1993.
Gutman, G., G., Ohring, and J. H. Joseph, Interaction between the geobotanic state and climate: A suggested approach and a test with a zonal model, *J. Atmos. Sci*., *41*, 2663–2678, 1984.
Huffman, G. J., R. F. Adler, B. Rudoff, U. Schneider, and P. R. Keehn, Global precipitation estimates based on a technique for combining satellite-based estimates, rain gauge analysis and NWP model precipitation estimates, *J. Clim*., *8*(2), 1284–1295, 1995.
Joseph, J. H., W. J. Wiscombe, and J. A. Weinman, The Delta-Eddington approximation for radiative flux transfer, *J. Atmos. Sci*., *33*, 2452–2459, 1976.
King, M. D., Harshvardhan, Comments on "The parameterization of radiation for numerical weather prediction and climate models," *Mon. Weather Rev*., *113*, 1832–1833, 1985.
Lacis, A. A., and J. E. Hansen, A parameterization for the absorption of solar radiation in the Earth's atmosphere, *J. Atmos. Sci*., *31*, 118–133, 1974.
Lean, J., and P. R. Rowntree, A GCM simulation of the impact of Amazonian deforestation on climate using improved canopy representation, *Q. J. R. Meteorol. Soc*., *119*, 509–530, 1993.
Lettau, H., K. Lettau, and L. C. B. Molion, Amazonia's hydrologic cycle and the role of atmospheric recycling in assessing deforestation effects, *Mon. Weather Rev*., *107*(3), 227–238, 1979.
Manabe, S., Climate and the ocean circulation, 1, The atmospheric circulation and the hydrology of the earth's surface, *Mon. Weather Rev*., *97*, 739–774, 1969.
Milly, P. C. D., and K. A. Dunne, Sensitivity of the global water cycle to the water-holding capacity of land, *J. Clim*., *7*, 506–526, 1994.
Nicholson, S. E., M. B. Ba, and J. Y. Kim, Rainfall in the Sahel during 1994, *J. Clim*., *9*(7), 1673–1676, 1996.
Nobre, C. A., P. J. Sellers, and J. Shukla, Amazonian deforestation and regional climatic change, *J. Clim*., *4*, 957–988, 1991.
Pal, J., and E. Eltahir, On the relationship between spring and summer soil moisture and summer precipitation over the Midwest, paper presented at 13th Conference on Hydrology, Am. Meteorol. Soc., Long Beach, Calif., 1997.
Raddatz, R. L., Prairie agroclimate boundary-layer model: A simulation of the atmosphere crop-soil interface, *Atmos. Ocean*., *31*(4), 399–419, 1993.
Reynolds, R. W., and T. M. Smith, Improved global sea surface temperature analyses, *J. Clim*., *7*, 929–948, 1994.
Rodgers, C. D., Some extension and applications of the new random model for molecular band transmission, *Q. J. R. Meteorol. Soc*., *94*, 99–102, 1968.
Rodriguez-Iturbe, I., D. Entekhabi, and R. L. Bras, Nonlinear dynamics of soil moisture at climate scales, 1, Stochastic analysis, *Water Resour. Res*., *110*, 1487–1494, 1991.
Sasamori, T., A numerical study of atmospheric and soil boundary layers, *J. Atmos. Sci*., *27*, 1122–1137, 1970.
Savenije, H., New definitions for moisture recycling and the relationship with land-use changes in the Sahel, *J. Hydrol*., *167*, 57–78, 1995.
Segal, M., and R. W. Arritt, Nonclassical mesoscale circulations caused by surface sensible heat-flux gradients, *Bull. Am. Meteorol. Soc*., *73*, 1593–1604, 1992.
Srinivasan, J., S. Gadgil, and P. J. Webster, Meridional propagation of large-scale monsoon convective zones, *Meteorol. Atmos. Phys*., *52*, 15–35, 1993.
Walker, J., and P. R. Rowntree, The effect of soil moisture on circulation and rainfall in a tropical model, *Q. J. R. Meteorol. Soc*., *103*, 29–46, 1977.
Williams, E., and N. Renno, An analysis of the conditional instability of the tropical atmosphere, *Mon. Weather Rev*., *121*, 21–36, 1993.
Yeh, T.-C., R. T. Wetherald, and S. Manabe, The effect of soil moisture on the short-term climate and hydrology change—a numerical experiment, *Mon. Weather Rev*., *112*, 474–490, 1984.
Zdunkowski, W. G., J. Paegle, and J. P. Reilly, The effect of soil moisture upon the atmospheric and soil temperature near the air-soil interface, *Arch. Meteorol. Geophys. Bioklimatol*., *Ser. A*, *24*, 245–268, 1975.
Zheng, X., The response of a moist zonally symmetric atmosphere to subtropical surface temperature perturbation, *Q. J. R. Meteorol. Soc*., in press, 1998.
Zheng, X., and E. A. B. Eltahir, The role of vegetation in the dynamics of West African monsoons, *J. Clim*., in press, 1998.

E. A. B. Eltahir and X. Zheng, Ralph M. Parsons Laboratory, Department of Civil and Environmental Engineering, Massachusetts Institute of Technology, Cambridge, MA 02139. (e-mail: eltahir@mit.edu)

(Received June 5, 1997; revised November 24, 1997;
accepted December 1, 1997.)